Journal of Proteomics xxx (xxxx) xxx–xxx

Contents lists available at ScienceDirect

Journal of Proteomics

journal homepage: www.elsevier.com/locate/jprot

Improvement of ubiquitylation site detection by Orbitrap mass spectrometry

Lennart van der Wal[a,1], Karel Bezstarosti[a,1], Karen A. Sap[a,b], Dick H.W. Dekkers[a], Erikjan Rijkers[a], Edwin Mientjes[c], Ype Elgersma[c], Jeroen A.A. Demmers[a,*]

[a] Proteomics Center, Erasmus University Medical Center, Wytemaweg 80, 3015 CN Rotterdam, The Netherlands
[b] Department of Cell Biology and Histology, Academic Medical Center, Meibergdreef 9, 1105 AZ Amsterdam, The Netherlands
[c] Department of Neuroscience, Erasmus University Medical Center, Wytemaweg 80, 3015 CN Rotterdam, The Netherlands

ARTICLE INFO

Keywords:
Ubiquitin
Ubiquitinome
Posttranslational modification (PTM)
diGly peptide
Immunopurification
Orbitrap mass spectrometry

ABSTRACT

Ubiquitylation is an important posttranslational protein modification that is involved in many cellular events. Immunopurification of peptides containing a K-ε-diglycine (diGly) remnant as a mark of ubiquitylation combined with mass spectrometric detection has resulted in an explosion of the number of identified ubiquitylation sites. Here, we present several significant improvements to this workflow, including fast, offline and crude high pH reverse-phase fractionation of tryptic peptides into only three fractions with simultaneous desalting prior to immunopurification and better control of the peptide fragmentation settings in the Orbitrap HCD cell. In addition, more efficient sample cleanup using a filter plug to retain the antibody beads results in a higher specificity for diGly peptides and less non-specific binding. These relatively simple modifications of the protocol result in the routine detection of over 23,000 diGly peptides from HeLa cells upon proteasome inhibition. The efficacy of this strategy is shown for lysates of both non-labeled and SILAC labeled cell lines. Furthermore, we demonstrate that this strategy is useful for the in-depth analysis of the endogenous, unstimulated ubiquitinome of in vivo samples such as mouse brain tissue. This study presents a valuable addition to the toolbox for ubiquitylation site analysis to uncover the deep ubiquitinome.

Significance: A K-ε-diglycine (diGly) mark on peptides after tryptic digestion of proteins indicates a site of ubiquitylation, a posttranslational modification involved in a wide range of cellular processes. Here, we report several improvements to methods for the isolation and detection of diGly peptides from complex biological mixtures such as cell lysates and brain tissue. This adapted method is robust, reproducible and outperforms previously published methods in terms of number of modified peptide identifications from a single sample. In-depth analysis of the ubiquitinome using mass spectrometry will lead to a better understanding of the roles of protein ubiquitylation in cellular events.

1. Introduction

The conjugation of the 8.5 kD protein ubiquitin to target proteins to mark them for proteasomal degradation is one of the key processes in cellular proteostasis. In this process the C-terminal carboxyl group of ubiquitin forms a covalent isopeptide bond with the ε-amino group of a lysine residue of the target protein. Ubiquitin is attached in a signaling cascade in which three enzyme types play a role, i.e. E1, E2 and E3 ubiquitin ligases [1,2]. Also, the ubiquitin moiety can be attached to another ubiquitin module, leading to the formation of branched polyubiquitin structures [1,3].

Although the initial discovery of ubiquitin was related to its role in mediating proteasomal degradation, it has become clear that protein mono- and polyubiquitylation is also involved in many proteasome-independent processes such as lysosomal degradation, DNA repair signaling, coordinating the cellular localization of proteins, activating and inactivating proteins and modulating protein-protein interactions [4]. The observation that proteins involved in ubiquitin signaling are often mutated in diseases such as cancer and neurodegenerative disorders illustrates the importance of ubiquitin in various key cellular processes [4,5].

Mass spectrometry has become the method of choice for the analysis of the cellular proteome over the past decade. Near complete proteomes representing thousands of different proteins from any biological source material can now be identified within a reasonable amount of time. While a mass spectrometric analysis is qualitative by nature, the use of

* Corresponding author.
E-mail address: j.demmers@erasmusmc.nl (J.A.A. Demmers).
URL: https://www.proteomicscenter.nl (J.A.A. Demmers).
[1] Equal contribution.

https://doi.org/10.1016/j.jprot.2017.10.014
Received 27 July 2017; Received in revised form 25 October 2017; Accepted 31 October 2017
1874-3919/ © 2017 The Author(s). Published by Elsevier B.V. This is an open access article under the CC BY license (http://creativecommons.org/licenses/BY/4.0/).

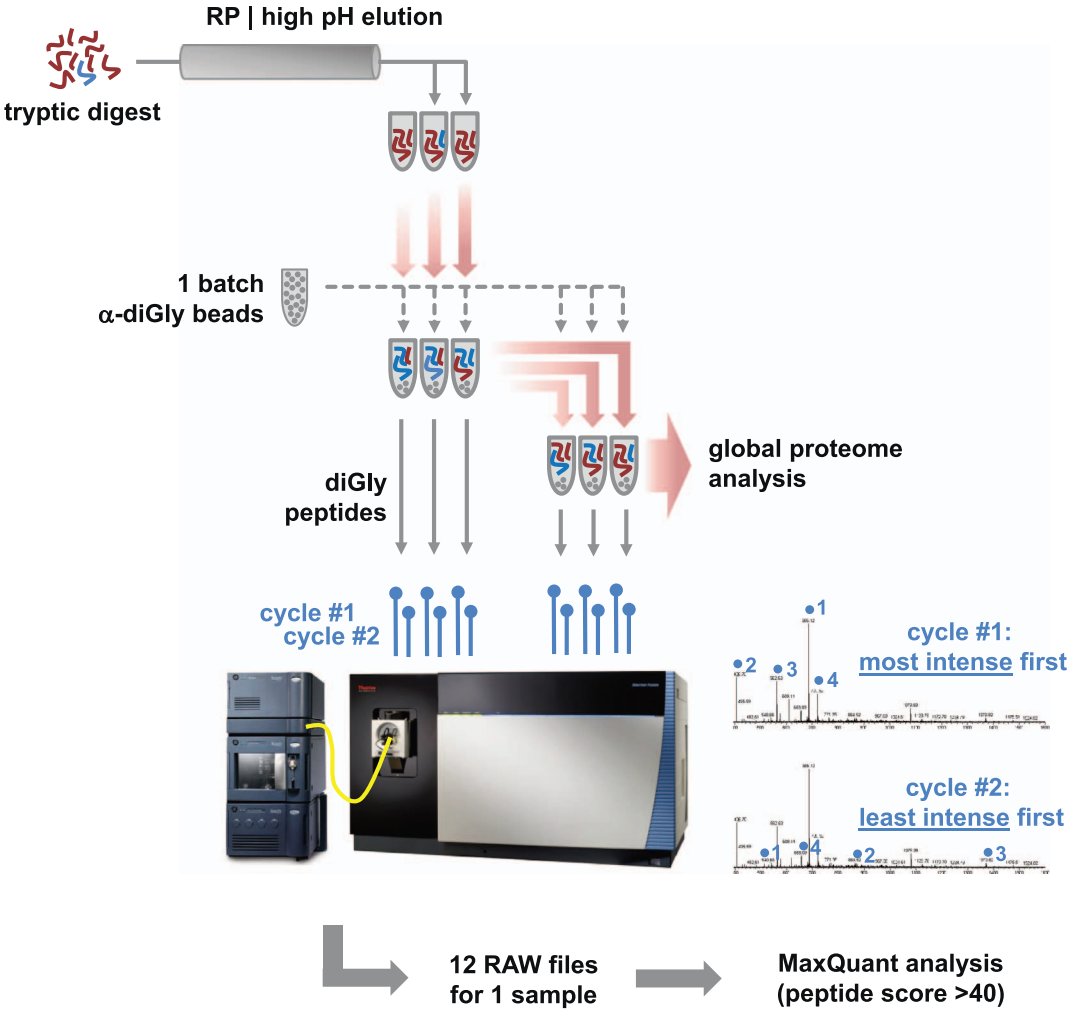

Fig. 1. Overview of the experimental approach. Samples are prepared, trypsinized and fractionated into three fractions using reverse-phase chromatography with high pH elution. One batch of commercial α-diGly peptide antibody beads is split into six equal fractions and the three peptide fractions are then loaded on three of the beads fractions. The diGly peptides are immunopurified, eluted and collected, and the flowthrough is subsequently transferred to the three remaining fresh beads fractions. The collected diGly peptides are analyzed by mass spectrometry on a Lumos Orbitrap mass spectrometer in a two-tier system consisting of one cycle in which the most intense peaks are first selected for peptide fragmentation and the next cycle in which the least intense peaks are selected first. The complete set of nLC-MS/MS runs are then analyzed using MaxQuant.

metabolic or chemical labeling can be used to add a robust quantification element to the analysis. Also, mass spectrometry is an indispensable tool for the analysis of protein posttranslational modifications (PTMs), ranging from small chemical moieties such as phosphorylation to complex glycan structures and small proteins such as ubiquitin and SUMO, with diverse biological functions.

Due to the nature of the mass spectrometric analysis, enrichment steps are necessary when measuring modified proteins or proteolytic peptides in order to cope with the generally relatively low stoichiometry of modified peptides compared to their non-modified counterparts. A range of specific methods have been developed to enhance the analysis of various PTMs such as phosphorylation, methylation, acetylation, ubiquitylation, etc.

Due to the multifaceted and important roles of ubiquitin, there is a great interest in the development of analytical methods for the (mass spectrometric) detection of protein ubiquitylation [6]. The use of mass spectrometry for the analysis of protein ubiquitylation has resulted in an explosion of the number of identified ubiquitylation sites in human, murine, *Drosophila* and yeast proteins over the past five years [7–12]. A major leap forward was presented by the development of an enrichment strategy based on immunoprecipitation using highly specific antibodies against the K-ε-GG (also referred to simply as diglycine or diGly) remnant motif that is produced upon tryptic digestion of ubiquitylated proteins [13,14].

This highly effective enrichment strategy has been used to investigate endogenous ubiquitylation sites in human cell lines [14], whether or not including fractionation of the immunoenriched peptides using isoelectric focusing or strong cation exchange (SCX) chromatography [10]. Adaptations to such protocols have been described by Udeshi and coworkers, who included fractionation of digested lysates based on SCX chromatography prior to immunoaffinity enrichment in a study to the effect of proteasome inhibition by MG132 and deubiquitinase inhibition by PR619 on ubiquitination sites in human Jurkat cells [11] and several improvements of this method, including optimized antibody and peptide input requirements, antibody cross-linking and improvement of basic reverse-phase offline fractionation prior to enrichment [15]. Recently, a method was described to quantitatively compare the ubiquitinomes from mouse tissue in a multiplexed manner using isobaric tagging with TMT [16].

Here, we describe a modified workflow to enrich for and detect diGly peptides originating from ubiquitylated proteins using immunopurification. Using a combination of several relatively simple modifications in the sample preparation and mass spectrometric detection protocols, we now routinely detect over 23,000 diGly modified peptides in a single sample of cells treated with proteasome inhibitors. We show the efficacy of this strategy for lysates from both non-labeled

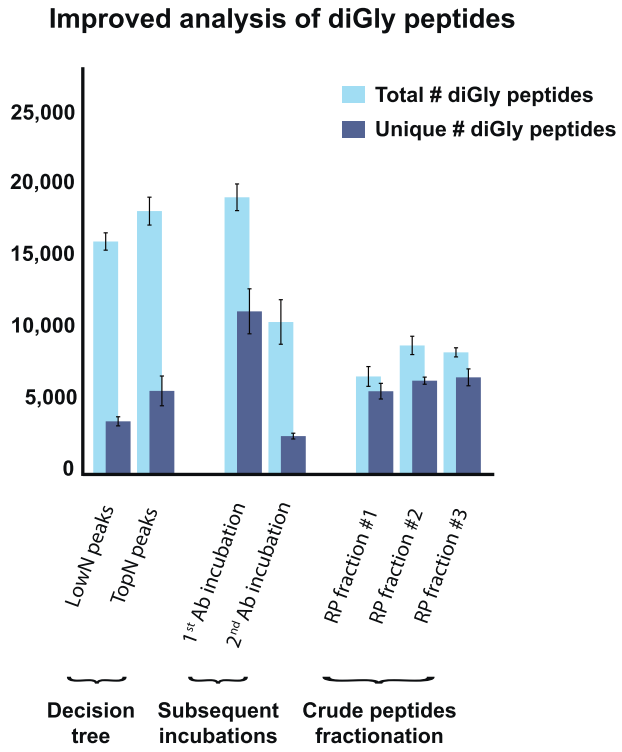

Fig. 2. Numbers of diGly peptides detected for each of the three improvement steps. The amount of unique diGly peptides per variable parameter in each improvement step is shown in dark blue; the total number of diGly peptides including those detected in multiple fractions, in both 1st and 2nd incubation or in both peak intensity priority fragmentation regimes is shown in light blue. Unique peptides are defined as those that do not overlap between the different parameters of each improvement step (i.e., fractions, 1st or 2nd incubation, fragmentation regimes). Bars indicate standard deviation.

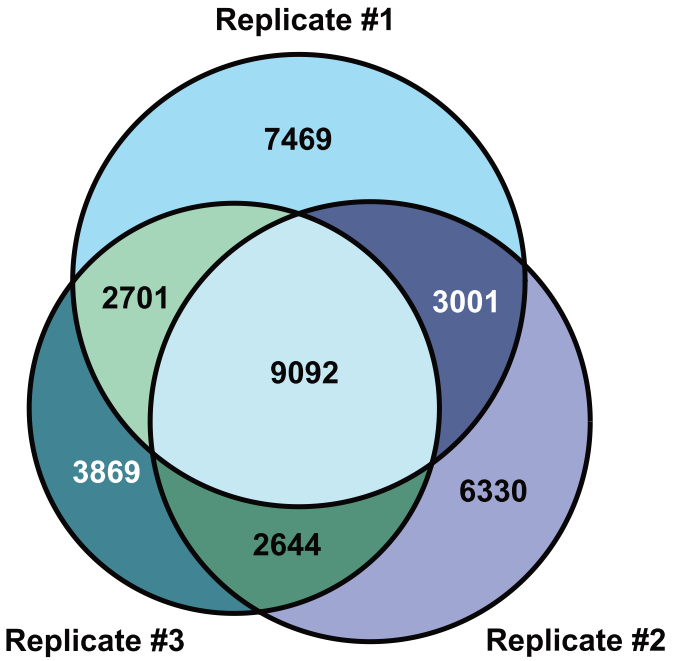

Fig. 3. DiGly peptides detected in three biological replicates of Bortezomib treated cells showing the amount of overlap between the runs.

and metabolically labeled (SILAC) mammalian cells. Furthermore, we demonstrate that this optimized strategy is also useful for the in-depth identification of the endogenous, unstimulated ubiquitinome of in vivo samples such as mouse brain tissue. As such, this study presents a valuable addition to the toolbox of the ubiquitylation site analysis for the identification of the deep ubiquitinome.

2. Material and methods

2.1. Sample preparation

Human cervical cancer cells (HeLa) and human osteosarcoma cells (U2OS) were grown in Dulbecco's Minimal Eagle Medium (DMEM) supplemented with 10% fetal bovine serum (FBS; heat inactivated, Gibco) and 100 units/ml penicillin/streptomycin. For SILAC experiments, cells were cultured in specially formulated DMEM (Thermo) lacking conventional Arginine and Lysine, supplemented with 10% dialyzed FBS (Sigma), 100 units/ml penicillin/streptomycin and glutamax (Gibco). SILAC cells were labeled with either conventional Lysine and Arginine (Sigma; referred to as 'Light'), Lysine-4 (4,4,5,5-D_4) and Arginine-6 ($^{13}C_6$) or Lysine-8 ($^{13}C_6$;$^{15}N_2$) and Arginine-10 ($^{13}C_6$;$^{15}N_4$) (Cambridge Isotope Laboratories; referred to as 'Medium' or 'Heavy', respectively). Cells were grown in this medium for at least 6 doublings before expansion and treatment.

After treatment with 10 μM Bortezomib (UBPbio) or an equivalent volume of DMSO as a mock treatment for 8 h, cells were washed with PBS, dissociated using 1% trypsin/EDTA and pelleted. Cell lysis was performed in 50 mM Tris-HCl (pH 8.2) with 0.5% sodium deoxycholate (DOC). Briefly, cells were incubated with the buffer and then boiled and sonicated for 10 min using a Bioruptor (Diagenode). Protein quantitation was performed using the colorimetric absorbance BCA protein assay kit (Thermo). Proteins were reduced using 5 mM 1,4-dithiothreitol for 30 min at 50 °C and subsequently alkylated using 10 mM iodoacetamide for 15 min in the dark. Proteins were first digested for 4 h with Lys-C (Wako Pure Chemicals; 1:200 enzyme:substrate ratio) and then overnight with trypsin (Thermo; 1:50 enzyme:substrate ratio) at 30 °C. Detergent was then removed by adding trifluoroacetic acid (TFA) to 0.5% and precipitated detergent was spun down at 10,000*g* for 10 min.

Mouse brain tissues were lysed using phase transfer surfactant (PTS; composed of 100 mM Tris-HCl (pH 8.5), 12 mM sodium DOC and 12 mM sodium N-lauroylsarcosinate) [17]. Briefly, tissues were incubated with the buffer and then boiled and sonicated for 10 min using a Bioruptor (Diagenode). Protein quantitation and digestion was performed as described above.

Peptide fractionation using high pH reverse-phase chromatography was performed using polymeric PLRP-S (300 Å, 50 μm, Agilent Technologies, part #PL1412-2K01) stationary phase material loaded into an empty Sep-Pak column cartridge (Waters). The stationary phase bed size was adjusted to the amount of protein digest that was to be fractionated. For 10 mg protein digest a 6 cm^3 Sep-Pak column cartridge filled with 0.5 g of stationary phase was used, resulting in a protein digest: stationary phase ratio of 1:50. The sample was loaded onto the column and washed with 10 column volumes of 0.1% TFA and 10 column volumes of milliQ H_2O. Next, peptides were eluted into three fractions with 10 column volumes of 10 mM ammonium formate solution (pH 10) and 7%, 13.5% and 50% acetonitrile (AcN), respectively. Fractions and flowthrough were subsequently dried to completeness by lyophilization.

For immunoprecipitation of diGly peptides, ubiquitin remnant motif (K-ε-GG) antibodies coupled to beads (PTMscan, Cell Signaling Technologies) were used. Each standard batch of beads was washed twice with PBS and then split into six fractions. The peptide fractions were dissolved in 1.4 ml IAP buffer (50 mM MOPS, 10 mM sodium phosphate and 50 mM NaCl, pH 7.2) and debris was spun down. The supernatant of the three fractions was incubated with beads for 2 h at 4 °C on a rotator unit. Subsequently, the supernatant was incubated again with the remaining bead fractions for 2 h at 4 °C. The supernatant was stored for further global proteome (GP) analysis.

Beads were transferred into a P200 pipette tip equipped with a GF/F

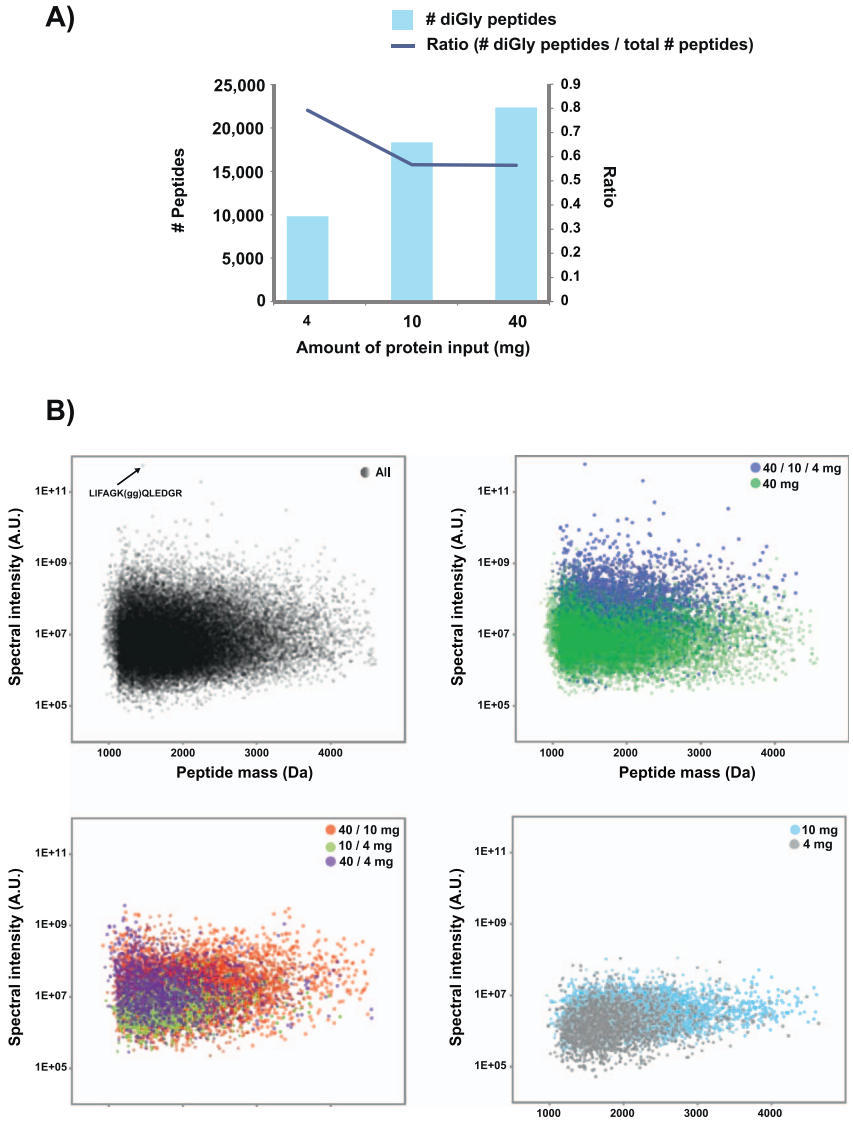

Fig. 4. A) Comparison of diGly peptides detected using increasing amounts of total protein input material. The ratio of numbers of diGly peptides to numbers of all peptides was determined to assess the enrichment efficiency, B) Plots of diGly peptide mass spectral intensities versus peptide masses showing the overlap between and unique identifications of the experiments with 4, 10 or 40 mg total protein input material.

filter plug (Whatman part #1825-021) to retain the beads. The beads were then washed 3 times with 200 µl of ice cold IAP buffer and subsequently 5 times with 200 µl of ice cold milliQ H_2O and peptides were eluted using 2 cycles of 50 µl 0.15% TFA. Finally, peptides were desalted using a C18 stage tip and dried to completeness using vacuum centrifugation.

2.2. NanoLC-MS

Mass spectra were acquired on an Oribtrap Tribrid Lumos mass spectrometer (Thermo) coupled to an EASY-nLC 1200 system (Thermo). Peptides were separated on an in-house packed 75 µM inner diameter column containing 50 cm Waters CSH130 resin (3.5 µm, 130 Å, Waters) with a gradient consisting of 2–28% (AcN, 0.1% FA) over 120 min at 300 nl/min. The column was kept at 50 °C in a NanoLC oven - MPI design (MS Wil GmbH). For all experiments, the instrument was operated in the data-dependent acquisition (DDA) mode. MS1 spectra were collected at a resolution of 120,000 with an automated gain control (AGC) target of 4E5 and a max injection time of 50 ms. The Thermo Tune software was set in such a way that in "highest intensity first" mode first the most intense ion was selected for MS/MS, then the second highest, etc. using the top speed method with a cycle time of 3 s. In contrast, in "lowest intensity first" mode the least intense ion was selected first, then the second lowest, etc. This option was discontinued from Tune version 2.1.1565.23 onward. Precursors were filtered according to charge state (2–7z), and monoisotopic peak assignment. Previously interrogated precursors were dynamically excluded for 60 s. Peptide precursors were isolated with a quadrupole mass filter set to a width of 1.6 Th. Ion trap MS2 spectra were collected at an AGC of 7E3, max injection time of 50 ms and HCD collision energy of 30%.

2.3. Data analysis

RAW files were analyzed using the MaxQuant software suite (version 1.5.4.1 or 1.5.6.0) [18]. Default search settings were selected with a few adaptations. Briefly, the enzyme specificity was set to trypsin, with the maximum number of missed cleavages raised to three. Lysine with a diGly remnant, oxidation of methionine and N-terminal acetylation were set as variable modifications. Carbamidomethylation of cysteine was set as a fixed modification. Searches were performed against a Uniprot fasta file composed of all *Homo sapiens* protein sequences (version June 2016) for the HeLa and U2OS experiments or all *Mus musculus* protein sequences (version July 2017) for the mouse brain experiments, combined with decoy and standard contaminant databases. The false discovery rate was set to 1%. The minimum score for diGly peptides was set to 40 (default); peptides identified with a C-terminal diGly modified lysine residue were excluded from further analysis. For the quantitative analysis of SILAC experiment files

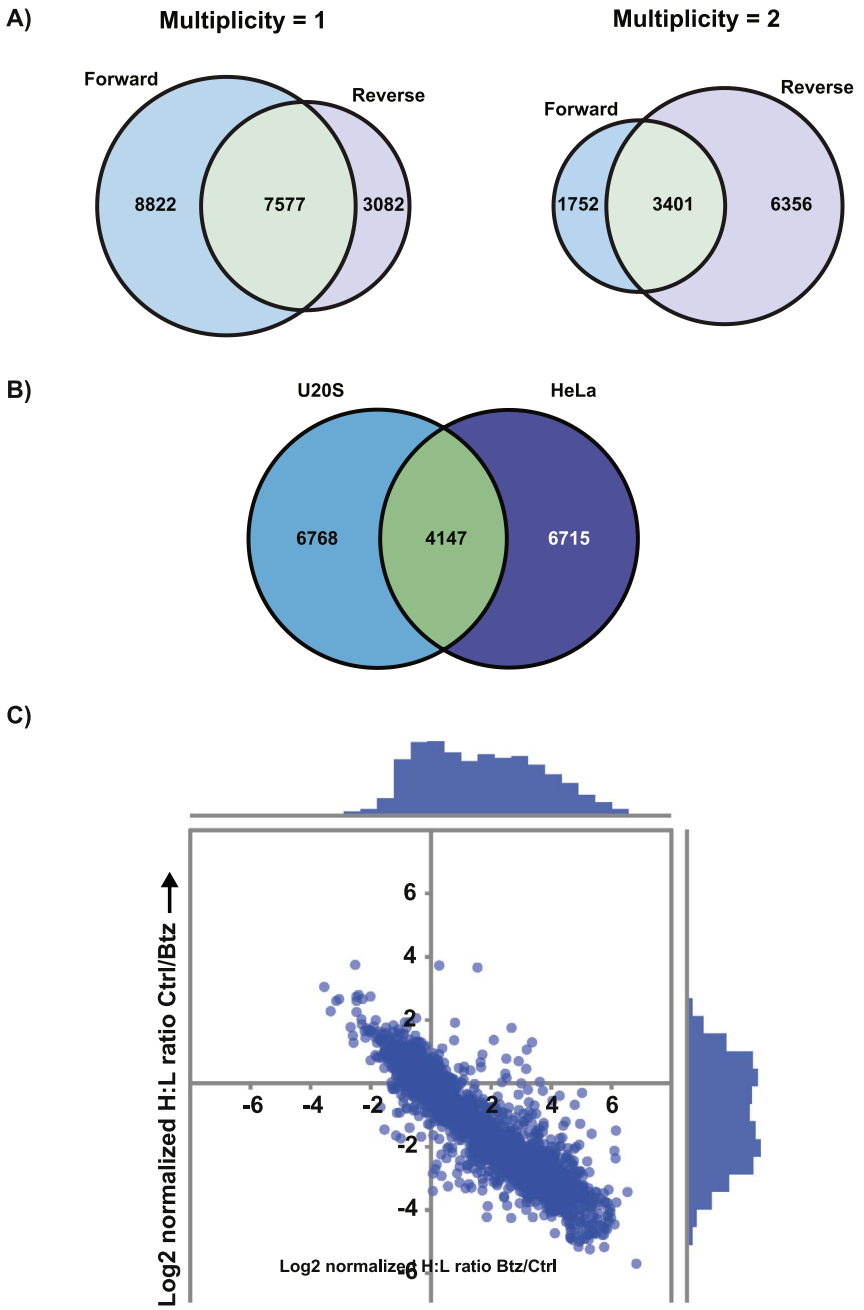

Fig. 5. Detection of diGly peptides in SILAC labeled cells. A) Numbers of peptides detected in the forward and reverse conditions of the SILAC labeled HeLa cells for multiplicity settings 1 and 2, B) Comparison of numbers of detected diGly peptides in SILAC labeled cells in different cell types, C) Scatterplot of diGly peptide SILAC ratios in Bortezomib (Btz) treated HeLa cells. Only peptides that were identified and quantified in both forward and reverse experiments are shown.

(multiplicity = 2) the minimum ratio count was set to 1. For assessment of the total number of diGly peptides identified from the SILAC experiments, searches were performed with the multiplicity reduced to 1, including the variable modifications Lysine-4 and Lysine-8 with their diGly modified counterparts and Arginine-6 and Arginine-10. Downstream analyses were performed with the Perseus package and with in-house developed software. Sequences from both PhosphoSitePlus and MaxQuant were converted to tables in a relational database (PostgreSQL) and manipulated as the respective sequence formats are somewhat different. Subsequently, they were (SQL) queried for overlapping sequences.

3. Results & discussion

We set out to develop and improve protocols for sample preparation and mass spectrometric detection of protein ubiquitylation sites in proteins from mammalian cultured cells. In order to boost protein ubiquitylation in cultured cells the chymotrypsin β5 proteasomal inhibitor Bortezomib was added for a few hours prior to cell lysis, protein isolation and subsequently tryptic digestion and mass spectrometric detection. Ubiquitylated proteins leave a diGly remnant on the ubiquitylated lysine when digested with trypsin and the mass difference caused by this motif can be used to unambiguously recognize ubiquitylation sites. Here, we describe a strategy that combines several improvements to state-of-the-art methods for the characterization of diGly peptides by nanoflow-liquid chromatography-mass spectrometry (nLC-MS/MS) which is outlined in Fig. 1. Briefly, the sample preparation procedure is optimized by introducing both crude peptide fractionation and subsequent incubation with fresh beads, while the mass spectrometric detection is improved by an adaptation of the duty cycle.

To reduce the complexity of the starting peptide pool we introduced a crude fractionation into three fractions using C18 reverse-phase chromatography and high pH elution. Basic reverse-phase fractionation was performed in the offline mode using a large Sep-Pak cartridge filled

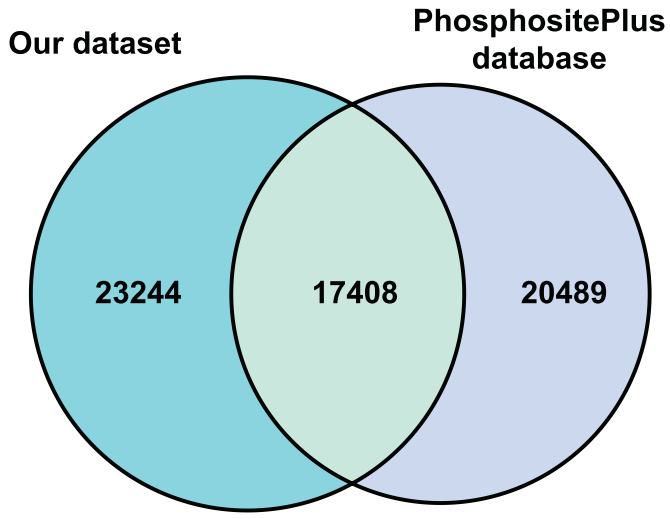

Fig. 6. Comparison of ubiquitylation sites identified in this data set versus those collected in the PhosphoSitePlus database.

Table 1
Gene Ontology (GO) analysis of proteins associated to up- and downregulated diGly peptides in HeLa and U2OS cells upon proteasome inhibition by Bortezomib.

HeLa cells			
Upregulated biological processes	p-Value	Benjamini score	# proteins
Nonsense mediated decay	2.2E − 38	2.37E − 35	61
Translational initiation	2.5E − 38	2.57E − 35	65
rRNA processing	3.2E − 28	2.3E − 25	69
Translation	9.6E − 26	5.8E − 23	72
mRNA stability	9.7E − 21	5.0E − 18	41
APC/C catabolism	1.6E − 19	7.3E − 17	35
Proteasome catabolism	1.9E − 19	7.5E − 17	56
Cell cycle related ubiquitylation	3.9E − 18	1.3E − 15	32
WNT signaling	3.8E − 16	9.3E − 14	34
Amino acid metabolism	3.1E − 15	7.5E − 13	25
NF kappaB signaling	4.5E − 15	1.0E − 12	28
Downregulated biological processes	p-Value	Benjamini score	# proteins
Nucleosome assembly	3.2E − 26	3.9E − 23	26
Translational initiation	1.5E − 8	9.0E − 6	13
Nonsense mediated decay	3.6E − 7	8.8E − 5	11
Cell-cell adhesion	2.1E − 5	2.9E − 3	13
Regulation of cell size	4.3E − 5	5.3E − 3	5

U2OS cells			
Upregulated biological processes	p-Value	Benjamini score	# proteins
Translational initiation	1.26E − 48	1.55E − 46	58
Nonsense mediated decay	1.11E − 42	2.42E − 39	50
rRNA processing	3.89E − 34	8.50E − 31	55
Translation	3.67E − 30	8.03E − 27	55
APC/C catabolism	2.85E − 25	6.24E − 22	31
Cell cycle related ubiquitylation	3.06E − 23	6.70E − 20	29
mRNA stability	1.50E − 22	3.27E − 19	32
Proteasome catabolism	3.64E − 22	7.96E − 19	42
NF kappaB signaling	1.11E − 18	2.42E − 15	24
WNT signaling	2.98E − 17	6.52E − 14	26
Amino acid metabolism	2.72E − 16	4.86E − 13	20
Downregulated biological processes	p-Value	Benjamini score	# proteins
Nucleosome assembly	1.4E − 24	5.3E − 22	19
Microtubule-based process	6.4E − 11	1.2E − 8	8
Keratinocyte differentiation	1.9E − 5	2.3E − 3	4
Cytoskeleton organization	3.4E − 5	3.1E − 3	7
H3K27Me3	2.1E − 4	1.3E − 2	3

with polymeric stationary phase to allow for the fractionation of up to 40 mg of input material. The acetonitrile percentage of the ammonium formate solution for elution into three fractions was optimized in such a way that every fraction contained similar peptide amounts. The desalting step that is normally performed before the basic reverse-phase fractionation when HPLC equipment is used can now be omitted, resulting in a significant decrease of the total time needed for the fractionation to only 45 min. Since these fractions showed only a very small overlap in peptide identifications, we decided to use these fractions for subsequent parallel diGly peptide IPs. α-K-ε-GG Antibodies coupled to beads were used according to the manufacturer's protocol (see Materials and methods). Although the exact amount of antibody per batch of beads is proprietary information, we use the same definition for one batch in this paper as the manufacturer does in order to avoid confusion. One batch of beads was divided into six smaller batches and peptides were incubated with these small bead batches twice in a sequential manner. In normal mode top *N* data dependent acquisition (DDA) analysis, *N* peaks from the MS1 spectrum are selected for fragmentation. This is done starting with the highest intensity peak, then the second highest intense peak, etc. However, a variation to this theme is to start with the least intense peaks and move on towards the higher intense peaks. The rationale behind this selection procedure is that extremely low abundant peptides will then be fragmented as well. To obtain higher ubiquitinome coverage, the highest first and lowest first peak intensity fragmentation regime runs from separate nLC-MS/MS experiments of one sample are then combined during the data analysis step. Altogether, this leads to a total amount of twelve nLC-MS/MS runs per sample while making use of only one batch of antibody beads. The improvements for each of the different steps will now be described in more detail.

Table 2
Overlap of diGly peptide data sets from experiments with varying amounts of total protein input material.

Total protein input amount	# diGly peptides
Present in all analyses	4553
Detected only in 10 and 40 mg experiments	5818
Detected only in 40 mg experiment	9963
Detected only in 4 and 10 mg experiments	1233
Detected only in 4 and 40 mg experiments	1614
Detected only in 10 experiment	5896
Detected only in 4 mg experiment	1761

The crude fractionation into three distinct fractions strategy reduces the sample complexity per fraction, with comparable amounts of diGly peptides per fraction identified (Fig. 2). The numbers of diGly peptides that were unique in each fraction (dark blue) are high with respect to the total number of diGly peptides in those fractions, indicating that the quality of the peptide separation is very high. It is expected that the diGly peptides, like the non-modified peptides from the same fraction, in the late eluting fractions are generally more hydrophobic. Sequence analysis of the diGly peptides for each of these fractions did not show any bias for diGly site context motifs (Supplementary Fig. 1).

In addition, ~2500 unique diGly peptides in were identified in a second IP incubation in addition to the first IP incubation using the flowthrough of the first IP with fresh antibody beads (Fig. 2). There was no apparent difference between the first and second IP in terms of diGly peptide properties, such as amino acid sequence, hydrophobicity, etc. The target specificity of this enrichment step was high, with a ratio between the numbers of diGly peptides over the total amount of peptides identified of 0.59.

Finally, the 'least intense precursor first' strategy produced over four thousand unique diGly peptides that were not detected when using the regular DDA protocol (Fig. 2).

Of all diGly peptides identified over three biological replicate experiments, 9092 were present in all of them, while almost 17,438 were present in at least two out of three replicates (Fig. 3). Reports in the literature on ubiquitylation profiling typically report around ten thousand ubiquitylation sites identified in a typical experiment (e.g.,

[10,16]). Thus, the method described here explores the ubiquitinome in more depth and in a reproducible manner.

For a complete list of identified diGly peptides see Supplementary Table 1.

The amount of input material for IPs was found to influence the ultimate number of diGly peptide identifications to a great extent. An IP performed with 4 mg of input material produced 9803 diGly peptide identifications, while the ratio of diGly peptide to total peptide identification numbers was high at 0.80 (Fig. 4A). Analyses of 10 mg protein input produced 18,427 diGly identifications, with a diGly peptide to total peptide ratio of 0.57. These results suggest that the available binding sites on the antibody beads may reach saturation when higher amounts of input material are used, or that highly abundant diGly peptides such as for instance the K48 modified tryptic peptide LIFAGK (diGly)QLEDGR of ubiquitin mask lowly abundant diGly peptides to a higher extent when more input material is used. Interestingly, in these lower input samples relatively higher amounts of diGly peptide identifications were found in the least intensity peaks first runs when compared to the regular, i.e. highest intensity peaks first, runs. It is possible that the higher sample input leads to increased peak intensities for diGly peptides, which in turn allows these peptides to be picked up in the regular Top N analysis. This would then lead to increased detection of peptides with ubiquitylation sites of low stoichiometry, but would at the same time increase the detection of background non-diGly peptides. When the spectral intensities of diGly peptides are plotted with respect to their masses it is obvious that the overlapping peptides between the analyses of different sample input amounts are largely peptides of relatively high intensities (Fig. 4B). Although there is quite some overlap between the 10 mg and 40 mg analyses, almost 10,000 diGly peptides were identified exclusively in the 40 mg preparation and > 5000 exclusively in the 10 mg preparation (Table 2). Only a minor fraction was identified exclusively in the 4 and/or 10 mg preparations and these peptides are mainly of (very) low abundance as based on their spectral intensities. Overall, the intensity range of diGly peptides spans almost eight orders of magnitude. It should be noted that no replicates were taken in this experiment and it is expected that the overlap would increase in that case.

For comparison purposes ubiquitinome analyses of untreated HeLa cells were performed. In a duplicate experiment that includes the improvements described above with 10 mg total protein input 7816 diGly peptides were identified (Supplementary Table 2). This number is a severe reduction compared to analyses of cells treated with proteasome inhibitors and fits with earlier observations in untreated cells where 30–40% of the total number of peptides found in treated cells were identified.

In order to illustrate the power of this improved method for ubiquitylation site analysis we also performed a quantitative SILAC analysis on the ubiquitinomes of Bortezomib treated HeLa cells versus non-treated cells. Biological replicates of each sample were analyzed in a light and heavy label swap SILAC experiment and samples were prepared and analyzed as described earlier using two batches of beads for the forward and reverse experiment. Again, of all peptides identified over 55% were diGly peptides. The overlap of diGly peptides detected in two independent experiments is depicted in Fig. 5A. In total, we detected 19,481 unique diGly peptides, while 7577 of these were detected in both experiments. In the quantitative analysis (SILAC settings or multiplicity 2) relatively large differences were observed in the numbers of diGly peptides identified exclusively in the forward condition (i.e., Bortezomib treated cells in the heavy channel, control cells in the light channel) versus those identified exclusively in the reverse condition (i.e., Bortezomib treated cells in the light channel, control cells in the heavy channel): 1752 compared to 6356. We suspect that this is due to the difficulties that the MaxQuant software has with the identification and quantitation of peptides that have measurable intensities (almost) exclusively in the heavy channel accompanied by extremely low intensities or even complete absence in the light channel. It is expected that this phenomenon occurs at a large scale when novel ubiquitylation sites are induced as a result of proteasome inhibition. The 'requantify' option in MaxQuant apparently only partially corrects for this. No major differences were observed between different cell types in terms of numbers of identified diGly peptides (Fig. 5B).

The far majority of diGly peptides are being upregulated upon Bortezomib treatment with > 65% of the peptides having H:L ratios of > 1.5 (Fig. 5C). Due to inhibition of the proteasome, proteins that are sent to the proteasome for degradation will now be accumulated instead, with proteins involved in highly active biological processes such as cell cycle regulation and transcription being enriched. Further GO analysis revealed an enrichment of additional cellular processes like protein catabolism and ubiquitylation, translation and non-sense mediated decay (Table 1). Notably, stress response proteins were highly upregulated and we have previously shown in *Drosophila* that this is because of protein biosynthesis rather than accumulation of non-degradable proteins [12]. The upregulation of diGly peptides of ubiquitin itself indicates an increase in the formation of all polyubiquitin chains (Supplementary Table 3).

We then compared the data generated by our method to publicly available repositories of ubiquitylation sites. The PhosphoSitePlus database (www.phosphosite.org) was used as the reference database, because this is one of the most extensive repositories of this kind. Surprisingly, only 45% of the sites found in our data set overlapped with those in the PhosphoSitePlus database, while > 20,000 of the observed ubiquitylation sites in our data set were not covered in this repository (Fig. 6; Supplementary Table 4). This indicates that the method described here reaches an unprecedented depth of ubiquitinome coverage.

Finally, we investigated the effectiveness of this method for the application of ubiquitylation site analysis in in vivo tissue samples. To assess this, we extracted approx. 32 mg protein from mouse brain tissue. It should be noted that no proteasome inhibitors or any other methods to boost overall protein ubiquitylation were applied. Using the experimental setup described here we identified 10,871 unique diGly peptides in this sample (Supplementary Table 5). Given that the diGly peptides identified here represent endogenous ubiquitylation sites with no externally imposed imbalance because of proteasome inhibition, we suspect that many of these ubiquitylation sites are actually signaling events, which is in line with ideas hypothesized by others [4,19,20].

4. Conclusions

We report several improvements for a method to enrich, immunopurify and identify peptides with diGly remnants representing sites of protein ubiquitylation. The numbers of identified peptides indicate a depth of analysis that is to our knowledge unprecedented in the literature. The adaptations of original procedures to analyze these modifications include 1) fractionation of the total peptide input prior to the specific immunoprecipitation of diGly peptides and 2) a more efficient decision tree in the Thermo Tune software workflow to optimize the Orbitrap mass spectrometer settings for the detection of these often extremely low abundant peptides. Furthermore, more efficient wash steps to decrease non-specific binding to the antibody beads resulted in higher overall diGly peptide vs non-modified peptide ratios. It should be noted here that in many reports in the literature numbers of identified diGly peptides reported are derived from accumulated analyses or experiments. The numbers presented here represent identified diGly peptides from a single sample and, therefore, only a single experiment. Also, the method is suitable for the detection of high amounts of endogenous ubiquitylation sites in mouse tissue samples. In conclusion, this method is robust, reproducible and outperforms previously published methods in terms of number of modified peptide identifications.

Supplementary data to this article can be found online at https://doi.org/10.1016/j.jprot.2017.10.014.

Transparency document

The Transparency document associated with this article can be found, in online version.

Acknowledgements

This work is part of the project “Proteins at Work”, a program of the Netherlands Proteomics Centre financed by The Netherlands Organization for Scientific Research (NWO) as part of the National Roadmap Large-Scale Research Facilities (project number 184.032.201).

Notes

The authors declare no conflict of interest.

The mass spectrometry proteomics data have been deposited to the ProteomeXchange Consortium via the PRIDE partner repository with the dataset identifier PXD007101.

References

[1] M.J. Clague, S. Urbé, Ubiquitin: same molecule, different degradation pathways, Cell 143 (2010) 682–685, http://dx.doi.org/10.1016/j.cell.2010.11.012.
[2] A. Ciechanover, The ubiquitin-proteasome proteolytic pathway, Cell 79 (1995) 13–21, http://dx.doi.org/10.1016/0092-8674(94)90396-4.
[3] F. Ohtake, H. Tsuchiya, The emerging complexity of ubiquitin architecture, J. Biochem. (2016) mvw088, , http://dx.doi.org/10.1093/jb/mvw088.
[4] D. Komander, M. Rape, The ubiquitin code, Annu. Rev. Biochem. 81 (2012) 203–229, http://dx.doi.org/10.1146/annurev-biochem-060310-170328.
[5] S. Bergink, S. Jentsch, Principles of ubiquitin and SUMO modifications in DNA repair, Nature 458 (2009) 461–467, http://dx.doi.org/10.1038/nature07963.
[6] J. Peng, D. Schwartz, J.E. Elias, C.C. Thoreen, D. Cheng, G. Marsischky, J. Roelofs, D. Finley, S.P. Gygi, A proteomics approach to understanding protein ubiquitination, Nat. Biotechnol. 21 (2003) 921–926, http://dx.doi.org/10.1038/nbt849.
[7] S.A. Wagner, P. Beli, B.T. Weinert, C. Schölz, C.D. Kelstrup, C. Young, M.L. Nielsen, J.V. Olsen, C. Brakebusch, C. Choudhary, Proteomic analyses reveal divergent ubiquitylation site patterns in murine tissues, Mol. Cell. Proteomics 11 (2012) 1578–1585, http://dx.doi.org/10.1074/mcp.M112.017905.
[8] V. Iesmantavicius, B.T. Weinert, C. Choudhary, Convergence of ubiquitylation and phosphorylation signaling in rapamycin-treated yeast cells, Mol. Cell. Proteomics 13 (2014) 1979–1992, http://dx.doi.org/10.1074/mcp.O113.035683.
[9] A.E.H. Elia, A.P. Boardman, D.C. Wang, E.L. Huttlin, R.A. Everley, N. Dephoure, C. Zhou, I. Koren, S.P. Gygi, S.J. Elledge, Quantitative proteomic atlas of ubiquitination and acetylation in the DNA damage response, Mol. Cell 59 (2015) 867–881, http://dx.doi.org/10.1016/j.molcel.2015.05.006.
[10] S.A. Wagner, P. Beli, B.T. Weinert, M.L. Nielsen, J. Cox, M. Mann, C. Choudhary, A proteome-wide, quantitative survey of in vivo ubiquitylation sites reveals widespread regulatory roles, Mol. Cell. Proteomics 10 (2011) M111.013284-M111.013284, , http://dx.doi.org/10.1074/mcp.M111.013284.
[11] N.D. Udeshi, D.R. Mani, T. Eisenhaure, P. Mertins, J.D. Jaffe, K.R. Clauser, N. Hacohen, S.A. Carr, Methods for quantification of in vivo changes in protein ubiquitination following proteasome and deubiquitinase inhibition, Mol. Cell. Proteomics 11 (2012) 148–159, http://dx.doi.org/10.1074/mcp.M111.016857.
[12] K.A. Sap, K. Bezstarosti, D.H. Dekkers, O. Voets, J.A. Demmers, Quantitative proteomics reveals extensive remodeling of the ubiquitinome after perturbation of the proteasome by dsRNA mediated subunit knockdown, J. Proteome Res. (2017), http://dx.doi.org/10.1021/acs.jproteome.7b00156.
[13] G. Xu, J.S. Paige, S.R. Jaffrey, Global analysis of lysine ubiquitination by ubiquitin remnant immunoaffinity profiling, Nat. Biotechnol. 28 (2010) 868–873, http://dx.doi.org/10.1038/nbt.1654.
[14] W. Kim, E.J. Bennett, E.L. Huttlin, A. Guo, J. Li, A. Possemato, M.E. Sowa, R. Rad, J. Rush, M.J. Comb, J.W. Harper, S.P. Gygi, Systematic and quantitative assessment of the ubiquitin-modified proteome, Mol. Cell 44 (2011) 325–340, http://dx.doi.org/10.1016/j.molcel.2011.08.025.
[15] N.D. Udeshi, T. Svinkina, P. Mertins, E. Kuhn, D.R. Mani, J.W. Qiao, S.A. Carr, Refined preparation and use of anti-diglycine remnant (K-epsilon-GG) antibody enables routine quantification of 10,000s of ubiquitination sites in single proteomics experiments, Mol. Cell. Proteomics 12 (2013) 825–831, http://dx.doi.org/10.1074/mcp.O112.027094.
[16] C.M. Rose, M. Isasa, A. Ordureau, M.A. Prado, S.A. Beausoleil, M.P. Jedrychowski, D.J. Finley, J.W. Harper, S.P. Gygi, Highly multiplexed quantitative mass spectrometry analysis of ubiquitylomes, Cell Systems (2016), http://dx.doi.org/10.1016/j.cels.2016.08.009.
[17] N. Sugiyama, T. Masuda, K. Shinoda, A. Nakamura, M. Tomita, Y. Ishihama, Phosphopeptide enrichment by aliphatic hydroxy acid-modified metal oxide chromatography for nano-LC-MS/MS in proteomics applications, Mol. Cell. Proteomics 6 (2007) 1103–1109, http://dx.doi.org/10.1074/mcp.T600060-MCP200.
[18] J. Cox, M. Mann, MaxQuant enables high peptide identification rates, individualized p.p.b.-range mass accuracies and proteome-wide protein quantification, Nat. Biotechnol. 26 (2008) 1367–1372, http://dx.doi.org/10.1038/nbt.1511.
[19] W. Kim, E.J. Bennett, E.L. Huttlin, A. Guo, J. Li, A. Possemato, M.E. Sowa, R. Rad, J. Rush, M.J. Comb, J.W. Harper, S.P. Gygi, Systematic and quantitative assessment of the ubiquitin-modified proteome, Mol. Cell 44 (2011) 325–340, http://dx.doi.org/10.1016/j.molcel.2011.08.025.
[20] S.E. Kaiser, B.E. Riley, T.A. Shaler, R.S. Trevino, C.H. Becker, H. Schulman, R.R. Kopito, Protein standard absolute quantification (PSAQ) method for the measurement of cellular ubiquitin pools, Nat. Methods 8 (2011) 691–696, http://dx.doi.org/10.1038/nmeth.1649.